UCSF
UC San Francisco Previously Published Works

Title

An OX40/OX40L interaction directs successful immunity to hepatitis B virus

Permalink

https://escholarship.org/uc/item/3hz7k14x

Journal

Science Translational Medicine, 10(433)

ISSN

1946-6234

Authors

Publicover, Jean
Gaggar, Anuj
Jespersen, Jillian M
et al.

Publication Date

2018-03-21

DOI

10.1126/scitranslmed.aah5766

Peer reviewed

An OX40/OX40L interaction directs successful immunity to hepatitis B virus

Jean Publicover[1,2,*], Anuj Gaggar[1,2,*,†], Jillian M. Jespersen[1,2,*], Ugur Halac[1,2,‡], Audra J. Johnson[1,2], Amanda Goodsell[1,2], Lia Avanesyan[3,4], Stephen L. Nishimura[5], Meghan Holdorf[6], Keith G. Mansfield[7], Joyce Bousquet Judge[7], Arya Koshti[6], Michael Croft[8], Adil E. Wakil[3,4], Philip Rosenthal[2,9,10], Eric Pai[1,2], Stewart Cooper[2,3,4], and Jody L. Baron[1,2,§]

[1]Department of Medicine, University of California, San Francisco (UCSF), San Francisco, CA 94143, USA

[2]UCSF Liver Center, UCSF, San Francisco, CA 94143, USA

[3]Liver Immunology Laboratory, California Pacific Medical Center Research Institute, San Francisco, CA 94115, USA

4Division of General and Transplant Hepatology, California Pacific Medical Center Research Institute, San Francisco, CA 94115, USA

5Department of Pathology, UCSF, San Francisco, CA 94143, USA

6Novartis Institute for Biomedical Research, Emeryville, CA 94619, USA

7Discovery and Investigative Pathology, Novartis Institute for Biomedical Research, Cambridge, MA 02139, USA

8La Jolla Institute for Allergy and Immunology, 9420 Athena Circle, La Jolla, CA 92037, USA

9Department of Pediatrics, UCSF, San Francisco, CA 94143, USA

10Department of Surgery, UCSF, San Francisco, CA 94143, USA

Abstract

Depending on age of acquisition, hepatitis B virus (HBV) can induce a cell-mediated immune response that results in either cure or progressive liver injury. In adult-acquired infection, HBV antigens are usually cleared, whereas in infancy-acquired infection, they persist. Individuals infected during infancy therefore represent the majority of patients chronically infected with HBV (CHB). A therapy that can promote viral antigen clearance in most CHB patients has not been developed and would represent a major health care advance and cost mitigator. Using an age-dependent mouse model of HBV clearance and persistence in conjunction with human blood and liver tissue, we studied mechanisms of viral clearance to identify new therapeutic targets. We demonstrate that age-dependent expression of the costimulatory molecule OX40 ligand (OX40L) by hepatic innate immune cells is pivotal in determining HBV immunity, and that treatment with OX40 agonists leads to improved HBV antigen clearance in young mice, as well as increased strength of T cell responses in young mice and adult mice that were exposed to HBV when they were young and developed a CHB serological profile. Similarly, in humans, we show that hepatic OX40L transcript expression is age-dependent and that increased OX40 expression on peripheral CD4+ T cells in adults is associated with HBV clearance. These findings provide new mechanistic understanding of the immune pathways and cells necessary for HBV immunity and identify potential therapeutic targets for resolving CHB.

INTRODUCTION

Hepatitis B virus (HBV) chronically infects ~300 million people and results in about 1 million deaths annually by causing liver failure and primary liver cancer [hepatocellular carcinoma (HCC)] (1). Adult patients who were infected before age 5 represent the major global reservoir because infants clear HBV at much lower rates than adults. In contrast to children, adults mount a strong and diverse adaptive immune response to HBV, which leads to viral clearance by mechanisms that are poorly understood (2–7). Because this strong adaptive immune response has been associated with sustained remission of liver disease and a lower risk for liver failure and HCC, discovery of mechanisms that tilt the immune response in patients with chronic HBV (CHB) infection toward a functional cure would open a gateway for developing definitive treatments.

To explore mechanisms that underlie HBV antigen clearance and the age-dependent divergent disease outcomes during acute hepatitis B (AHB) infection, our laboratory developed a transgenic mouse model that faithfully mimics key aspects of the age-dependent immunological differences in human HBV clearance and persistence (8, 9). In this model, we use HBV transgenic mice crossed with mice genetically deficient in the recombinase RAG-1 ($Rag1^{-/-}$), which is required to generate mature B and T cells (10). These mice express HBV antigens (HBVEnvRag$^{-/-}$) or intact virus (HBVRplRag$^{-/-}$) in the liver, in the absence of an adaptive immune system that would otherwise be immunologically tolerant toward HBV antigens. Adoptive transfer of 10^8 HBV-naïve, syngeneic splenocytes from wild-type (WT) C57BL/6 or genetically modified mice reconstitutes the immune system and allows for the evaluation of contributions of cellular and soluble mediators in HBV pathogenesis (11). Adoptive transfer of adult splenocytes into adult HBV transgenic $Rag1^{-/-}$ mice (HBVtgRag$^{-/-}$; including HBVEnvRag$^{-/-}$ and HBVRplRag$^{-/-}$ strains), leads to an effective immune response with disease kinetics that are comparable to those seen in adult humans experiencing acute, self-limited infection. Specifically, these reconstituted adult mice generate a diverse HBV-specific T cell response and a serological profile [HBV core antibody (HBcAb)$^+$, surface antibody (HBsAb)$^+$, and surface antigen (HBsAg)$^-$] that precisely mirrors immune responses seen in the peripheral blood of patients who clear HBV infection. Conversely, adoptive transfer of adult splenocytes into young HBVtgRag$^{-/-}$ mice leads to an immune response, disease kinetics, and a serological profile (HBcAb$^+$, HBsAb$^-$, and HBsAg$^+$) mirroring those seen in the peripheral blood of patients who develop CHB (8). This model has provided an opportunity to uncover mechanisms leading to effective immunity and to experimentally modulate ineffective responses toward HBV clearance.

Data generated using this model, and our parallel studies in humans, have demonstrated that hepatic lymphoid organization and the competency of immune priming within the hepatic microenvironment pivotally guide HBV-specific T cell diversity, HBsAb seroconversion, and viral control (8, 9). Our data support a model whereby effective HBV immunity involves intrahepatic T follicular helper (T_{FH}) cell priming, leading to local production of interleukin-21 (IL-21) at sites where IL-21 is necessary for promoting effective antiviral responses by CD8$^+$ T cells and B cells, which, in turn, lead to HBV clearance. The ineffective immune response generated in young mice and humans is primed in a hepatic microenvironment with diminished lymphoid organization and greatly diminished IL-21 production and T_{FH} number. The implications of this model suggest that age-dependent expression of molecules on hepatic antigen-presenting cells (APCs) facilitate effective T and B cell responses to HBV. Here, we explore this hypothesis and examine the expression and role of the costimulatory molecule OX40L on hepatic APCs and of its cognate receptor OX40 on T lymphocytes in age-dependent HBV immunity.

RESULTS

OX40 ligand expression on hepatic APCs is age-dependent, and age-dependent expression of OX40 on liver-derived CD4$^+$ T cells is observed during acute hepatitis

To further elucidate the cells and molecules necessary for effective hepatic immune priming, we surveyed APCs from the livers of uninfected young and adult mice for expression of

costimulatory molecules known to be important in the initiation and expansion of T cell responses. Here, we focused on the expression of the tumor necrosis factor (TNF) receptor (TNFR)/TNF superfamily members OX40 and its partner OX40 ligand (OX40L) because of their known ability to control diverse aspects of immune function, including the regulation of conventional CD4$^+$ and CD8$^+$ T cell responses (12–15). These studies revealed age-dependent differences in the expression of OX40L on hepatic macrophages, monocytes, and dendritic cells (DCs). Specifically, real-time polymerase chain reaction (PCR) analysis of isolated nonparenchymal liver cells from $Rag1^{-/-}$ mice demonstrated a sevenfold increase of OX40L mRNA expression in 8- to 11-week-old (adult) mice compared to 3-week-old (young) mice (Fig. 1A). Strikingly, expression of hepatic OX40L begins increasing to adult levels by age 5 weeks, at the same time that the immune response to HBV in our model begins to convert to the adult profile (Fig. 1A). To determine which cells in the liver express OX40L, nonparenchymal cells from the livers of adult and young $Rag1^{-/-}$ mice were isolated and enriched for myeloid cells. We then analyzed and purified the various cell populations using flow cytometric analysis and fluorescence-activated cell sorting (FACS). This revealed significant age-dependent differences in the expression of OX40L on resident macrophages ($P = 0.0005$ and $P < 0.0001$), monocytes/monocyte-derived macrophages ($P = 0.0035$ and $P = 0.0128$), and DCs ($P = 0.0087$ and $P = 0.0134$) derived from livers of adult and young mice (Fig. 1B and fig. S1E), without age-dependent differences in the percentage or absolute numbers of these hepatic APCs (Fig. 1C; representative FACS plots and absolute numbers in fig. S1). Consistent with the flow cytometry data, we demonstrated greater relative expression of OX40L mRNA on flow-sorted APCs from both adult $Rag1^{-/-}$ and WT mice (Fig. 1D and fig. S2A). Thus, whereas the number of hepatic macrophages, monocytes, and DCs is not age-dependent, the expression of OX40L on these hepatic APCs increases with age.

Expression of OX40L is limited to CD45$^+$ leukocytes, and accordingly, we did not detect expression of OX40L on liver sinusoidal endothelial cells, hepatocytes, or stellate cells (fig. S2B). Notably, although the presence of the HBV transgene (without adoptive transfer of splenocytes) does not influence OX40L expression in the young mice, it does increase the expression of OX40L in adult mice relative to $Rag1^{-/-}$ mice (fig. S2C). The age-dependent expression of OX40L is specific to the liver, because we observed similar (age-independent) expression in the spleen and lymph nodes (fig. S2D). In addition, 12 weeks after the adoptive transfer of splenocytes, adult (HBVtgRag$^{-/-}$) mice that generated an effective immune response to HBV (HBsAg clearance and HBsAb production) maintain higher expression of OX40L compared to adult mice that encountered HBV antigens when they were young and developed ineffective immunity ("chronic" HBVtgRag$^{-/-}$; fig. S2E). This increased expression of OX40L is specific to the liver, because splenocytes from these animals had similar expression of OX40L as compared to untransferred and chronic controls (fig. S2F).

To demonstrate biological effects of the age-dependent expression of OX40L in the liver, we analyzed the expression of its receptor, OX40, on hepatic lymphoid cells derived from young and adult HBVEnvRag$^{-/-}$ mice at the peak of the HBV-specific T cell response 8 days after adoptive transfer of adult splenocytes. Percentages and absolute numbers of CD4$^+$ T cells ($P < 0.0001$ and $P < 0.0001$) and OX40$^+$ T cells ($P < 0.0001$ and $P = 0.0001$), as well as CD4$^+$

TFH cells ($P = 0.0035$) and OX40$^+$ CD4$^+$ T$_{FH}$ ($P = 0.008$) cells, were significantly increased in the recipient adult mice compared to the young mice (Fig. 1, E and F; and fig. S3, A to D). In addition, we observed that a greater percentage of all CD4$^+$ T cells in the liver of adult recipients were OX40$^+$, as compared to the percentage of all CD4$^+$ T cells expressing OX40 in the liver of young recipient mice, thus demonstrating that the increase in OX40$^+$ CD4$^+$ T cells and T$_{FH}$ cells is not just a consequence of increased CD4$^+$ T cells in general (Fig. 1G). In contrast, there were no relative differences in OX40 expression on CD8$^+$ T cells. This expansion of OX40$^+$ CD4$^+$ T cells in the liver of adult mice was also reflected in peripheral blood mononuclear cells (PBMCs) (fig. S3E). These results suggest that the age-dependent expression of OX40L on liver APCs contributes to the efficacy of priming and expansion of hepatic CD4$^+$ T cells, including T$_{FH}$ cells, in response to HBV.

Adoptive transfer of adult *Ox40*$^{-/-}$ splenocytes into adult HBVtgRag$^{-/-}$ mice alters the effectiveness of the immune response to HBV

To further test this hypothesis and the biological significance of OX40/OX40L interactions in influencing the immune response to HBV, we compared the response and disease outcome in both lineages of adult HBVtgRag$^{-/-}$ mice after adoptive transfer of splenocytes from WT (*Ox40*$^{+/+}$) mice or *Ox40*$^{-/-}$ mice. Strikingly, expression of OX40 on splenocytes was necessary for clinical hepatitis (Fig. 2, A to C, and fig. S4A), clearance of HBsAg (Fig. 2D and fig. S4B), and HBsAb seroconversion (Fig. 2E and fig. S4C). Interferon-γ (IFN-γ) enzyme-linked immunospot (ELISpot) analysis of liver lymphocytes also revealed that expression of OX40 on donor splenocytes is necessary to generate diverse primary and memory HBV-specific hepatic CD4$^+$ and CD8$^+$ T cell responses (Fig. 2, F and G). The expression of OX40 was also necessary for the HBV-specific increase in hepatic CD4$^+$ cells, including T$_{FH}$, as well as the hepatic IL-21 expression that is crucial for effective HBV immunity (Fig. 2, H to J, and fig. S4D), as we have previously shown (8).

We next studied the livers of HBVRplRag$^{-/-}$ mice 7 days and 8 to 24 weeks after adoptive transfer of WT or *Ox40*$^{-/-}$ splenocytes, compared with untransferred HBVRplRag$^{-/-}$ mice, to address the mechanisms of HBsAg clearance from the blood of HBVtgRag$^{-/-}$ mice in our adoptive transfer model. All mice that received WT splenocytes developed clinical hepatitis by day 7 [increased alanine aminotransferase (ALT); Fig. 3A] and had established HBV immunity with undetectable HBsAg in the serum at 8 to 24 weeks (table S1); none of the mice that received *Ox40*$^{-/-}$ splenocytes developed clinical hepatitis or cleared HBsAg from the serum. Northern blot analysis was performed on total hepatic RNA to detect HBV envelope transcripts, and hepatic expression of HBsAg protein was determined by immunohistochemical staining. At day 7 after adoptive transfer, mice that received either WT ($P = 0.0082$ and $P = 0.0009$) or *Ox40*$^{-/-}$ ($P = 0.017$ and $P = 0.0035$) splenocytes both had a significant reduction of the 2.4- and 2.1-kb viral transcripts, respectively, detected relative to the hepatic steady-state transcript content in the untransferred mice, whereas at later time points (8 to 24 weeks), only the mice that received WT splenocytes had reduction of these viral transcripts ($P = 0.047$ and $P = 0.044$; Fig. 3, B, C, and E). This finding of differences in the reduction of viral transcripts may reflect the differences observed in hepatic IFN-γ production detected in the transferred mice (Fig. 2, F and G) and is consistent with the known mechanisms of noncytolytic inhibition of HBV replication by IFN-γ (16,

17). Immunohistochemical staining of liver for detection of HBsAg revealed expression of antigen in the livers of mice in all groups (Fig. 3, D and F).

Together, these results suggest that loss of HBsAg from the serum of mice that received WT splenocytes and produced HBsAb is largely a result of antibody-mediated antigen clearance (18), with some contribution of cytokine-mediated inhibition of viral transcription. Furthermore, the result that the mice that received $Ox40^{-/-}$ splenocytes do not clear serum HBsAg likely reflects both a lack of production of HBsAb (Fig. 2E and fig. S4C) and decreased cytokine production in the liver (Fig. 2, F and G).

$Ox40^{-/-}$ mice are not globally immunosuppressed but have been shown to generate selectively weaker CD4$^+$ T cell responses in some tissues (19). In our experiments, recipients of $Ox40^{-/-}$ splenocytes generated HBV responses that mirrored the ineffective immune response profiles of young HBVtgRag$^{-/-}$ mice (8) and young humans (20). Specifically, these mice developed mild hepatic inflammation and weaker HBV-specific T cell responses, displayed weaker inhibition of hepatic viral replication, and failed to generate HBsAb but did generate HBcAb (Fig. 2, A to G; Fig. 3, B, C, and E; and fig. S4, A to E). In addition, just like young WT mice and young HBV-naive humans, $Ox40^{-/-}$ mice also generated HBsAb in response to the human recombinant HBV vaccine (fig. S4F).

When adult HBVEnvRag$^{-/-}$ mice were given a blocking antibody directed against OX40L on days 0, 2, 4, and 6 after adoptive transfer of WT splenocytes, the early immune response and disease outcome paralleled the results demonstrated in adult HBVEnvRag$^{-/-}$ that received $Ox40^{-/-}$ splenocytes (Fig. 4). Specifically, the blocking antibody prevented clinical hepatitis (Fig. 4A and fig. S5A), significantly limited the expansion of hepatic CD4$^+$ T cells ($P < 0.0001$; fig. 4B), limited the diversity of the HBV-specific hepatic CD4$^+$ and CD8$^+$ T cell responses (Fig. 4C), and significantly decreased the hepatic expression of IL-21 ($P = 0.0054$; Fig. 4D). This early intervention of OX40L blockade in the first weeks of the immune response, however, was not able to significantly alter the long-term HBsAg clearance or HBsAb seroconversion (fig. S5, B and C). Thus, an OX40/OX40L interaction is crucial for effective HBV immunity and is likely required beyond the initial priming window.

An OX40 agonist can tilt the immune response toward HBV antigen clearance

In light of these findings, we tested the hypothesis that augmented signaling through OX40 in young mice could beneficially alter the HBV-specific immune response and disease outcome. Young HBVtgRag$^{-/-}$ mice received WT splenocytes and either an anti-OX40 agonistic antibody or an isotype control antibody. In contrast to the young mice that received the control antibody, young mice treated with the OX40 agonist developed mild hepatitis, displayed increases in the percentages and absolute numbers of CD4$^+$ T cells and T$_{FH}$ cells, generated a more diverse HBV-specific T cell response, and 50% cleared HBsAg from plasma (Fig. 5, A to D, and fig. S6, A and B). Analysis of the HBV-specific T cell responses in the OX40 agonist-treated young mice that cleared HBsAg revealed substantial differences in the strength and diversity of the T cell response compared with young mice that received the agonist and did not clear HBsAg (Fig. 5E). Intriguingly, none of the young mice that cleared HBsAg produced HBsAb (fig. S6E). The fact that these mice do not seem to produce

HBsAb likely reflects low CXCL13 expression in the livers of these young animals, which we have shown to be critical for hepatic B cell responses against HBV (9). This finding suggests that a strong, diverse T cell response might facilitate effective HBV control even in the absence of HBsAb production.

We then tested the hypothesis that signaling through OX40 could augment the HBV immune response in adult chronic HBVtgRag$^{-/-}$ mice that received WT splenocytes when they were 3 weeks of age and had developed the serological profile of an HBV-specific immune response that correlates with viral persistence. Specifically, 3-week-old HBVtgRag$^{-/-}$ mice received WT splenocytes and were allowed to age to 12 weeks. All mice were confirmed to have the serological profile of chronic inactive HBV, including no ALT rise, HBsAg persistence, and lack of HBsAb seroconversion. At 12 weeks after adoptive transfer, the mice received eight doses of either OX40 agonist antibody or isotype control antibody over 3 weeks (Fig. 5F), or three doses of either OX40 agonist or isotype control antibody, followed by an additional four doses beginning at week 24 after adoptive transfer (Fig. 5, G and H). Although the mice did not clear HBsAg or generate detectable HBsAb, both dosing schedules and both lines of transgenic mice treated with the OX40 agonist experienced transient hepatitis and had detectable HBV-specific T cell responses, whereas the mice treated with the isotype antibody did not (Fig. 5, F to H, and fig. S6, C and D).

Adult human liver shows greater OX40L expression than infant liver, and patients with AHB who clear the virus have significantly increased percentages of PBMC-derived CD4$^+$ T cells, a greater percentage of which express OX40

To assess the translational relevance of our findings, we analyzed relative expression of OX40L mRNA in paraffin-embedded uninfected human liver biopsy tissue from infant (ages 6 to 12 weeks) and adult livers and found that OX40L is expressed in an age-dependent manner in human liver (Fig. 6A), similar to that found in the mice. To assess the CD45$^+$ APCs in human liver, we analyzed the expression of the macrophage/monocyte selective markers CD14 and CD68 and observed no increase in these transcripts in adult livers compared to infant livers (fig. S7). This finding suggests that similar to mice, the number of hepatic macrophages and monocytes in humans is not age-dependent, whereas the expression of OX40L on these hepatic APCs increases with age.

To seek parallels between functional data from our mouse model and the HBV immune response in humans, we examined PBMC from HBV-infected and control patients for evidence of an association between CD4$^+$ T cell expression of OX40 and an effective immune response. These studies revealed that like adult mice, adult patients with AHB infection have increased numbers of CD4$^+$ T cells, and a greater percentage of these CD4$^+$ T cells express OX40 during the primary immune response compared to adult patients with CHB (Fig. 6C). Furthermore, this increase in circulating OX40$^+$ T cells in patients with AHB was not observed during the ineffective immune response that occurs in patients with CHB during a hepatitic flare or in patients with inactive CHB (Fig. 6, B and C, and fig. S8). Thus, such increases are distinctly observed in patients who clear HBV and are not seen in chronically infected patients with similar levels of serum HBV DNA and liver inflammation or in patients with inactive CHB (Fig. 6C). We did not detect a significant difference in the

percentage of circulating T_{FH} or $CD8^+$ T cells in these patient-derived peripheral blood samples (Fig. 6B).

DISCUSSION

Chronic infection with HBV afflicts up to 300 million people and is the world's leading cause of cirrhosis, liver failure, and HCC. Although CHB can usually be suppressed by long-term antiviral therapy, modern treatments must typically be taken indefinitely because they rarely induce durable immunity and lead to sustained HBsAg clearance. Definitive, more cost-effective therapies are urgently needed that can promote HBV antigen clearance and immunity and, ultimately, lowered risk of HCC and cirrhosis in the millions of people with CHB.

A clear mechanistic understanding of the events that lead to failed HBV immunity should facilitate the development of new therapeutics, but gaining this knowledge has been difficult. The primary obstacle to human research stems from the fact that most patients who fail to clear HBV were infected as infants or young children, years before infection became clinically evident. Therefore, the early events in immune activation to HBV in most patients cannot be studied contemporaneously. Thus, experiments aimed at understanding failed immunity to HBV, and uncovering new therapeutic approaches to modulate immunity, must primarily rely on animal models, coupled with focused experiments using blood and tissue from patients to validate the models, as developed here.

Using a mouse model of HBV infection that recapitulates the key dichotomous differences in HBV immunity between infection in early life and adulthood in humans, we show a critical role for age-dependent expression of OX40L by hepatic APCs in the initiation of an HBV immune response that leads to effective immunity. Our data firmly implicate diminished hepatic OX40L expression in young mice and young humans as playing a major role in the ineffective immune response that results in CHB. Furthermore, we also show that effective immunity to HBV, including IL-21 production by T_{FH}, a strong and diverse primary T cell response, HBsAb seroconversion, and HBsAg clearance, is OX40/OX40L-dependent. The HBV age-dependent aspect aside, our data are consistent with studies demonstrating a role for OX40/OX40L interaction in the expansion and maintenance of T cell responses against other viruses (12–15, 21–24).

As with all animal models of human disease, certain aspects of natural HBV infection are not recapitulated, for example, the mice are not naturally infected by HBV and do not form cccDNA (covalently closed circular DNA) but are producing transgenic HBV proteins and virions. In addition, in the HBV transgenic model, a naive immune system abruptly encounters hepatocytes expressing high levels of HBV antigen or virions. It is for these reasons that we went on to probe hepatic immunity and the immune response to HBV using cells and tissue from patients, guided by our findings in the mouse model.

These comparative studies of patients acutely and chronically infected with HBV additionally support that adults with CHB have impaired OX40/40L-dependent immunity, which has clear implications for potential therapies. Our demonstration that an OX40

agonist can tilt the immune response toward HBV clearance in young mice and in adult chronic mice that encountered antigen when they were young opens new avenues for treating CHB in humans. Preclinical studies using tumor models demonstrate that tumor-associated, antigen-specific CD8^{+} T cells increase in quantity after OX40 agonist immunotherapy, and OX40 agonists, plus and minus checkpoint blockade, lead to reduced tumor growth and improved overall survival (25–28). Our data suggest that the OX40/OX40L pathway is crucial for effective HBV immunity and that OX40 agonists have potential in definitively treating CHB by augmenting the virus-specific T cell response. However, similar to use in tumor models, OX40 agonists alone might not be sufficient to fully reprime the immune response to HBV. Thus, analogous to approaches for cancer immunotherapy, OX40 agonists for the treatment of CHB might be used either alone or in combination with other immune modulatory agents that target pathways that we and others have demonstrated to be important in the generation of an immune response that leads to viral control or tumor regression (8, 9, 11, 25–27, 29–34). Our data suggest that the OX40/OX40L pathway functions in natural hepatic immunity, which establishes its potential for therapeutic manipulation in treating CHB and a variety of other infectious, immune, and neoplastic liver diseases.

MATERIALS AND METHODS

Study design

We sought to elucidate mechanistic understanding of the immune pathways and cells necessary for HBV immunity and to identify potential therapeutic targets for resolving CHB. To accomplish this, studies were designed in five parts: (i) to identify age-dependent expression of costimulatory molecules on APCs from the livers of young and adult mice, which are known to be important in the initiation and expansion of T cell responses; (ii) to study the role of an identified receptor/ligand pair, OX40/OX40L, in an established transgenic mouse model that mimics key aspects of the age-dependent immunological differences in human HBV clearance and persistence; (iii) to test whether augmented signaling through OX40 in mice could beneficially alter the HBV-specific immune response and disease outcome; (iv) to test whether age-dependent differences in the expression of OX40L observed in mouse livers might be recapitulated in humans; and (v) to seek parallels between functional data from our mouse model and the HBV immune response in human PBMCs. For all mouse experiments, mice were age- and sex-matched (both sexes included) and were assigned randomly to the different experimental groups. Data collection was terminated at relevant clinical and biological time points. Mice were kept in microisolator cages in a specific pathogen–free facility, and the University of California, San Francisco (UCSF) Institutional Animal Care and Use Committee approved all animal experiments carried out in this study. For comparative studies using human cells and tissue, sample size was determined by matching the number of mice included for data generation in the respective experiments and/or the availability of pertinent, clinically annotated samples in our biorepository (6 to 24 individuals). No outlier analysis was performed. UCSF and California Pacific Medical Center institutional review boards approved all human studies. Primary data for all studies are in table S3.

Mice and experimental system

WT C57BL/6 mice were purchased from Jackson Laboratory. HBVEnvRag$^{-/-}$ and HBVRplRag$^{-/-}$ mice were previously described (11). Briefly, HBVEnvRag$^{-/-}$ mice were generated using HBV-Env$^+$ mice [lineage 107-5D; gift from F. Chisari, Scripps Research Institute (35)] backcrossed to *Rag1*$^{-/-}$ C57BL/6 mice for 15 generations. HBVEnvRag$^{-/-}$ mice contain the entire envelope (subtype ayw) protein-coding region under the constitutive transcriptional control of the mouse albumin promoter. HBVRplRag$^{-/-}$ mice were generated using HBV replication mice [lineage 1.3.46; gift from F. Chisari (36)] crossed to *Rag1*$^{-/-}$ C57BL/6 mice for 15 generations. HBVRplRag$^{-/-}$ mice contain a terminally redundant HBV DNA construct and produce infectious virus in their hepatocytes and in the proximal convoluted tubules of their kidneys. Young (3 to 4 weeks old, before weaning) or adult (8 to 12 weeks old) HBVtgRag$^{-/-}$ mice were given 10^8 syngeneic splenocytes pooled from adult (8 to 12 weeks) WT or mutant mouse strains in 0.5 ml of phosphate-buffered saline via tail vein injection. Mice were followed for plasma ALT using an ALT-L3K kit (Sekisui Diagnostics) on a Cobas Miras Plus analyzer (Roche Diagnostics). C57BL/6, *Ox40*$^{-/-}$ mice were generated at UCSF (37), but provided to us by M. Croft (La Jolla Institute for Allergy and Immunology).

HBV protein assays

Plasma was collected and assayed for the presence of HBsAg by using ETI-MAK-2 Plus (DiaSorin). HBsAg results are reported as positive or negative, determined by parameters programmed by DiaSorin in an ELx800 plate reader (BioTek). Total HBsAb was quantified by using ETI-AB-AUK PLUS and ABAU standard set (DiaSorin). Plasma from transferred HBVRplRag$^{-/-}$ mice was assayed for the presence of total HBcAb using ETI-AB-COREK PLUS (DiaSorin).

Cell preparations

Lymphocytes were isolated from the liver after perfusion and digestion. Briefly, mice were perfused via the inferior vena cava using digestion media [RPMI 1640 containing 5% fetal bovine serum (FBS), crude collagenase (0.2 mg/ml; Crescent Chemical), and DNase I (0.02 mg/ml; Roche Diagnostics)]. Livers were forced through a 70-μm filter using a syringe plunger, and debris was removed by centrifugation (30g for 3 min). Supernatants were collected and centrifuged for 10 min at 650g. Lymphocytes were isolated from the Percoll interface using a 60%:40% Percoll gradient. Myeloid fractions were isolated from the liver after 6 min of perfusion via the inferior vena cava using digestion media as above. Livers were chopped and further digested with liberase and DNase I (Roche Diagnostics) [1 Wünsch Units (WU) and 0.8 mg, respectively, in 10 ml of RPMI 1640 containing 5% FBS] for 30 min at 37°C in a shaking water bath. Livers were forced through a 70-μm filter, and debris was removed by centrifugation (30g for 3 min). Supernatants were collected and centrifuged for 10 min at 650g. Cells were isolated from the interface of a 25%:50% Percoll gradient.

Flow cytometry

Lymphocytes and myeloid cells were prepared as above. Cells were stained according to standard protocols with combinations of the following anti-mouse antibodies: OX40-APC (eBioscience; clone, OX86), CD4-FITC (eBioscience; clone, GK1.5), CD4-APC-Cy7 (BD Biosciences; clone, GK1.5), CD8–Pacific Orange (Life Technologies; clone, 5H10), CD8– Pacific Blue (BD Biosciences; clone, 53-6.7), TCRb–Pacific Blue (BD Biosciences; clone, H57-597), TCRb-PE (BD Biosciences; clone, H57-597), NK1.1-PE-Cy7 (eBioscience; clone, PK136), CD19–Alexa Fluor 700 (eBioscience; clone, ebio1D3), CD19-APCCy7 (BD Biosciences; clone, 1D3), CXCR5-biotin (BD Biosciences; clone, 2G8), OX40L-PE (eBioscience; clone, RM134L), F4/80-PE-Cy7 (eBioscience; clone, BM8), CD11b-PerCP-Cy5.5 (BD Biosciences; clone, M1/70), CD11c-APC (eBiosciences; clone, N418), major histocompatibility complex II–efluor 450(I-A/I-E) (eBioscience; clone, M5/114.15.2), Ly6g-PerCP-Cy5.5 (BD Biosciences; clone, 1A8), and Ly6c-AF700 (BD Biosciences, clone: AL-21). When applicable for biotinylated antibodies, cells were stained with secondary QDot 605–conjugated streptavidin (Life Technologies). Cells were analyzed using an LSR II flow cytometer (BD Biosciences) and FlowJo software (TreeStar) or sorted on an Aria III (BD Biosciences).

Enzyme-linked immunospot

IFN-γ ELISpot assays (BD Biosciences) were performed on unstimulated liver lymphocytes. Liver lymphocytes were prepared as described above. Peptide pool ELISpot assays were performed using IFN-γ ELISpot assays plated with lymphocytes from transferred animals combined 1:1 with $Rag1^{-/-}$ splenocytes to provide optimal APC stimulation. Fifteen-mer peptides were generated across the whole envelope protein with 11 overlapping amino acids between peptides (Sigma-Aldrich), and 12 to 14 sequential peptides were combined in seven pools. Cells were incubated with peptides at a final concentration of 5 μg/ml for each peptide. ELISpot was performed following the manufacturer's instructions (BD Biosciences). Later in our studies, we identified dominant and subdominant epitopes within the peptide pools and incubated with those identified peptides at a final concentration of 5 μg/ml (table S2).

OX40L blocking antibody and OX40 agonist

For specified experiments, HBVEnvRag$^{-/-}$ adult mice received intraperitoneal injection of 100 μg of OX40L blocking antibody (RM134L, BioXCell) or control immunoglobulin G (IgG) (purified rat IgG2b isotype control, UCSF Monoclonal Antibody Core Facility) on days 0, 2, 4, and 6 after adoptive transfer of adult WT splenocytes. Similarly, 3-week-old HBVEnvRag$^{-/-}$ mice received intraperitoneal injection of 150 μg of OX40 agonist antibody (OX86, BioXCell) or with control IgG (purified rat IgG1 isotype control, UCSF Monoclonal Antibody Core Facility) on days 0, 3, and 5 after adoptive transfer of adult WT splenocytes. For experiments treating mice confirmed to have the serological profile of CHB (adoptively transferred at 3 weeks of age; no early ALT rise, HBsAg$^+$, and HBsAb$^-$ and allowed to rest for 3 months), mice received an intraperitoneal injection of 150 μg of OX40 agonist antibody or with control IgG either on days 84, 87, 89 and 168, 171, 173, 175 after adoptive

transfer of adult WT splenocytes or three times per week for eight treatments starting on day 84 after adoptive transfer of adult WT splenocytes.

Liver hematoxylin and eosin histology

Liver tissue was fixed in 4% paraformaldehyde (PFA) or 10% formalin and embedded in paraffin blocks. Five-micrometer slices were cut. PFA- and formalin-fixed tissues were stained with hematoxylin and eosin (H&E) according to standard protocols by the Gladstone Histology and Light Microscopy Core and scored by a pathologist who was blinded to sample identity.

RNA extraction and real-time PCR

RNA isolated from lymphocytes was prepared using an RNeasy micro kit (Qiagen) with vortex and QIAshredder (Qiagen) disruption. RNA isolated from liver tissue was prepared using an RNeasy mini kit (Qiagen) using bead beat lysing (MP Biomedicals) and QIAshredder (Qiagen) disruption. cDNA was generated on 0.25 to 1.00 μg of RNA using a iScript cDNA synthesis kit (Bio-Rad). Real-time PCR was performed on 2.5 μl of cDNA product using iTaq Universal SYBR Green Supermix with ROX (Bio-Rad) and the following mouse gene primers: *Gapdh*, 5′-GGAGCGAGACCCCACTAACA-3′ (forward) and 5′-ACATACTCAGCACCGGCCTC-3′ (reverse); *Il21*, 5′-TCATCATTGACCTCGTGGCCC-3′ (forward) and 5′-ATCGTACTTCTCCACTTGCAATCC-3′ (reverse); and *Ox40l*, 5′-TCTGTGCTTCATCTATGTCTGC-3′ (forward) and 5′-CATCCTCACATCTGGTAACTGC-3′ (reverse). Real-time PCR was performed on the 7300 Real-Time PCR System (Applied Biosystems).

HBV transcript measurement by Northern blot

RNA was extracted from flash-frozen liver pieces collected 1, 8, or 24 weeks after adoptive transfer of HBVRplRag$^{-/-}$ recipient mice with either WT or *Ox40*$^{-/-}$ splenocytes using a modified TRIzol extraction (38). Briefly, 1 ml of TRIzol (Life Technologies) was added to 25 mg of tissue and homogenized at 6000 rpm for 30 s using the MagNA Lyser instrument (Roche). RNA was extracted into the aqueous phase with the addition of 0.2 ml of chloroform (Sigma-Aldrich) and precipitated in 0.5 ml of isopropanol (Sigma-Aldrich). The pellet was washed with 1 ml of 75% ethanol and resuspended in RNase-free water. Ten-microliter RNA samples were separated by denaturizing 1.2% agarose gel electrophoresis with reagents from the NorthernMax Kit (ThermoFisher) and transferred to a Nytron membrane using the TurboBlotter apparatus (Sigma-Aldrich). A DIG-labeled (−) strand HBV RNA probe was transcribed from Sca I–linearized pGEM3ZHBV plasmid with the DIG Northern Starter Kit (Sigma-Aldrich) according to the manufacturer's instructions. Hybridization at 68°C, washes, and detection with CDP-Star were carried out according to the DIG Wash and Block buffer set instructions (Sigma-Aldrich), and images were acquired with the Azure c300 system (Azure Biosystems). HBV envelope transcript abundance was quantitated using ImageJ software analysis (39) of HBV envelope large (2.4 kb) and middle/small (2.1 kb) RNA transcript band intensities detected on the Northern blots and normalized to detected 18*S* RNA band intensities for each sample.

HBsAg protein detection and scoring by immunohistochemistry

Liver tissue was collected 1, 8, or 24 weeks after adoptive transfer of HBVRplRag$^{-/-}$ mice with either WT or *Ox40*$^{-/-}$ splenocytes and fixed in 10% formalin for 24 hours. Fixed liver tissue was subsequently processed and embedded in paraffin following standard protocols. Paraffin blocks were sectioned at 5 μm, and immunohistochemistry for HBV surface antigen was performed on these formalin-fixed paraffin-embedded (FFPE) tissues. Briefly, molecular localization studies were conducted using a Ventana Discovery XT autostainer (Ventana Medical Systems, Roche Group). FFPE tissues were sectioned at 5 μm, bar-coded, and then placed in the autostainer for paraffin extraction and rehydration. A rabbit polyclonal antibody (Bio-Rad) was found to be specific for HBV surface antigen and was used at a final concentration of 1.3 μg/ml. Antigen retrieval (CC1 mild; Ventana Medical Systems), primary antibody dilution, incubation temperature and duration, detection technique, and 3,3′-diaminobenzidine (DAB) chromogen (ChromoMap DAB Kit, Ventana Medical Systems) were optimized on sections of HBV-infected positive control liver (Newcomer Supply) and included evaluation of isotype-matched irrelevant antibody controls, as well as known negative liver tissue. Slides were counterstained (hematoxylin, Ventana Medical Systems) and coverslipped (Micromount, Leica Biosystems). HBsAg expression was scored qualitatively by an unbiased pathologist using the following criteria: 0, no staining; 1, multifocal granular or diffuse staining in hepatocytes involving <25% of section; 2, granular or diffuse staining around centrilobular hepatocytes with no staining in portal regions; 3, diffuse positivity of hepatocytes restricted to the centrilobular region; granular cytoplasmic positivity in the remaining hepatocytes; 4, diffuse positivity of hepatocytes restricted to the centrilobular and mid zonal regions; granular cytoplasmic positivity in the remaining hepatocytes; and 5, diffuse positivity of all hepatocytes.

Patient samples and OX40L RNA expression

Twenty-four infants (6 to 12 weeks of age) were liver-biopsied to rule out biliary atresia at the UCSF Medical Center. Six of these patients were found to have biliary atresia, 6 had neonatal nonviral hepatitis, 10 were found to have a nonspecific liver disease diagnosis, including cholestasis and ductopenia, and 2 had an unknown diagnosis. Nine adult liver samples were obtained from donor livers before transplantation. RNA from FFPE tissue was extracted using the RNeasy FFPE kit (Qiagen) following the manufacturer's instructions. Isolated RNA (150 ng) was reverse-transcribed using the QuantiFast Probe assay (Qiagen) and amplified using specific probes and primers to human *GAPDH* and *OX40L* or using by the prime PCR probe assay (Bio-Rad) for *CD14, CD68*, and *GAPDH*.

PBMC were obtained from eight patients with confirmed AHB infection at the time of active hepatitis and confirmed subsequent viral clearance and HBsAb seroconversion, eight patients with confirmed CHB infection exhibiting a flare of disease (ALT rise), as well as six patients with confirmed CHB with inactive disease (normal ALT), and six healthy individuals. Cells were stained according to standard protocols with combinations of the following antihuman antibodies: TCRab-PE-Cy7 (BioLegend; clone, IP26), CD4-BV785 (BioLegend; clone, OKT4), OX40-PE [BioLegend; clone, Ber-ACT35 (ACT35)], ICOS–PerCP–eFluor 710 (eBioscience; clone, ISA-3), CXCR5-APCs (BD Biosciences; clone, RF8B2), CD8-BV570 (BioLegend; clone, RPA-T8), CD56-BV605 (BioLegend; clone,

HCD56), CD16-AF700 (BioLegend; clone, 3G8), and CD19-BV650 (BioLegend; clone, HIB19).

Acutely infected HBV patients had confirmed elevated viral loads ($6.3 \times 10^6 \pm 5.1 \times 10^6$ IU/ml), elevated ALT (146 to 2996 U/liter), HBsAg$^+$ and IgM core antibody–positive, and a clinical history of exposure. CHB patients exhibiting a flare in disease had confirmed elevated viral loads ($1.4 \times 10^7 \pm 5.1 \times 10^6$ IU/ml), elevated ALT (133 to 1307 U/liter), HBsAg$^+$, and known history of chronic infection. Chronic inactive HBV patients not on antiviral therapy had confirmed low ALT (16 to 32 U/liter) and confirmed viral loads (2453 ± 1262 IU/ml). Uninfected controls had confirmed low ALT (16 to 32 U/liter) and were HBsAg$^-$.

Statistical analysis

Statistics were performed using Prism (Graph Pad Software). Statistical significance was determined by two-tailed unpaired Student's t test (when two groups were compared), two-tailed paired Student's t test (for longitudinal analyses of the same mice), or Tukey's analysis of variance (ANOVA) multiple-comparison test (when more than two groups were compared). For significance of HBsAg clearance, in which one of two possible outcomes was compared (clearance versus no clearance), Fisher's chi-square test was used. For ordinal or ranked data (histology scores), the Mann-Whitney rank sum test was used. In all figures with multiple n, data are presented as means ± SEM. $P < 0.05$ was considered significant.

Supplementary Material

Refer to Web version on PubMed Central for supplementary material.

Acknowledgments

References

1. Lee WM. Hepatitis B virus infection. N. Engl. J. Med. 1997; 337:1733–1745. [PubMed: 9392700]

2. Nebbia G, Peppa D, Maini MK. Hepatitis B infection: Current concepts and future challenges. QJM. 2012; 105:109–113. [PubMed: 22252919]

3. Bertoletti A, Ferrari C. Innate and adaptive immune responses in chronic hepatitis B virus infections: Towards restoration of immune control of viral infection. Gut. 2012; 61:1754–1764. [PubMed: 22157327]

4. Dandri M, Locarnini S. New insight in the pathobiology of hepatitis B virus infection. Gut. 2012; 61(Suppl. 1):i6–i17. [PubMed: 22504921]

5. Chisari FV, Isogawa M, Wieland SF. Pathogenesis of hepatitis B virus infection. Pathol. Biol. (Paris). 2010; 58:258–266. [PubMed: 20116937]

6. Zhang Y, Cobleigh MA, Lian J-Q, Huang C-X, Booth CJ, Bai X-F, Robek MD. A proinflammatory role for interleukin-22 in the immune response to hepatitis B virus. Gastroenterology. 2011; 141:1897–1906. [PubMed: 21708106]

7. Yang PL, Althage A, Chung J, Maier H, Wieland S, Isogawa M, Chisari FV. Immune effectors required for hepatitis B virus clearance. Proc. Natl. Acad. Sci. U.S.A. 2010; 107:798–802. [PubMed: 20080755]

8. Publicover J, Goodsell A, Nishimura S, Vilarinho S, Wang Z-e, Avanesyan L, Spolski R, Leonard WJ, Cooper S, Baron JL. IL-21 is pivotal in determining age-dependent effectiveness of immune responses in a mouse model of human hepatitis B. J. Clin. Invest. 2011; 121:1154–1162. [PubMed: 21393863]

9. Publicover J, Gaggar A, Nishimura S, Van Horn CM, Goodsell A, Muench MO, Reinhardt RL, van Rooijen N, Wakil AE, Peters M, Cyster JG, Erle DJ, Rosenthal P, Cooper S, Baron JL. Age-dependent hepatic lymphoid organization directs successful immunity to hepatitis B. J. Clin. Invest. 2013; 123:3728–3739. [PubMed: 23925290]

10. Mombaerts P, Iacomini J, Johnson RS, Herrup K, Tonegawa S, Papaioannou VE. RAG-1-deficient mice have no mature B and T lymphocytes. Cell. 1992; 68:869–877. [PubMed: 1547488]

11. Baron JL, Gardiner L, Nishimura S, Shinkai K, Locksley R, Ganem D. Activation of a nonclassical NKT cell subset in a transgenic mouse model of hepatitis B virus infection. Immunity. 2002; 16:583–594. [PubMed: 11970881]

12. Croft M. Control of immunity by the TNFR-related molecule OX40 (CD134). Annu. Rev. Immunol. 2010; 28:57–78. [PubMed: 20307208]

13. Croft M, So T, Duan W, Soroosh P. The significance of OX40 and OX40L to T-cell biology and immune disease. Immunol. Rev. 2009; 229:173–191. [PubMed: 19426222]

14. Salek-Ardakani S, Moutaftsi M, Crotty S, Sette A, Croft M. OX40 drives protective vaccinia virus-specific CD8 T cells. J. Immunol. 2008; 181:7969–7976. [PubMed: 19017988]

15. Boettler T, Moeckel F, Cheng Y, Heeg M, Salek-Ardakani S, Crotty S, Croft M, von Herrath MG. OX40 facilitates control of a persistent virus infection. PLOS Pathog. 2012; 8:e1002913. [PubMed: 22969431]

16. Guidotti LG, Ishikawa T, Hobbs MV, Matzke B, Schreiber R, Chisari FV. Intracellular inactivation of the hepatitis B virus by cytotoxic T lymphocytes. Immunity. 1996; 4:25–36. [PubMed: 8574849]

17. Guidotti LG, Rochford R, Chung J, Shapiro M, Purcell R, Chisari FV. Viral clearance without destruction of infected cells during acute HBV infection. Science. 1999; 284:825–829. [PubMed: 10221919]

18. Gao Y, Zhang T-Y, Yuan Q, Xia N-S. Antibody-mediated immunotherapy against chronic hepatitis B virus infection. Hum. Vaccin. Immunother. 2017; 13:1768–1773. [PubMed: 28521640]

19. Kopf M, Ruedl C, Schmitz N, Gallimore A, Lefrang K, Ecabert B, Odermatt B, Bachmann MF. OX40-deficient mice are defective in Th cell proliferation but are competent in generating B cell and CTL responses after virus infection. Immunity. 1999; 11:699–708. [PubMed: 10626892]

20. Edmunds WJ, Medley GF, Nokes DJ, Hall AJ, Whittle HC. The influence of age on the development of the hepatitis B carrier state. Proc. Biol. Sci. 1993; 253:197–201. [PubMed: 8397416]

21. Huang L-R, Wohlleber D, Reisinger F, Jenne CN, Cheng R-L, Abdullah Z, Schildberg FA, Odenthal M, Dienes H-P, van Rooijen N, Schmitt E, Garbi N, Croft M, Kurts C, Kubes P, Protzer U, Heikenwalder M, Knolle PA. Intrahepatic myeloid-cell aggregates enable local proliferation of CD8+ T cells and successful immunotherapy against chronic viral liver infection. Nat. Immunol. 2013; 14:574–583. [PubMed: 23584070]

22. Salek-Ardakani S, Moutaftsi M, Sette A, Croft M. Targeting OX40 promotes lung-resident memory CD8 T cell populations that protect against respiratory poxvirus infection. J. Virol. 2011; 85:9051–9059. [PubMed: 21715499]

23. Song J, So T, Cheng M, Tang X, Croft M. Sustained survivin expression from OX40 costimulatory signals drives T cell clonal expansion. Immunity. 2005; 22:621–631. [PubMed: 15894279]

24. Zhang J-Y, Wu X-L, Yang B, Wang Y, Feng G-H, Jiang T-J, Zeng Q-L, Xu X-S, Li Y-Y, Jin L, Lv S, Zhang Z, Fu J, Wang F-S. Upregulation of OX40 ligand on monocytes contributes to early

virological control in patients with chronic hepatitis C. Eur. J. Immunol. 2013; 43:1953–1962. [PubMed: 23589118]

25. Triplett TA, Tucker CG, Triplett KC, Alderman Z, Sun L, Ling LE, Akporiaye ET, Weinberg AD. STAT3 signaling is required for optimal regression of large established tumors in mice treated with anti-OX40 and TGFβ receptor blockade. Cancer Immunol. Res. 2015; 3:526–535. [PubMed: 25627655]

26. Moran AE, Polesso F, Weinberg AD. Immunotherapy expands and maintains the function of high-affinity tumor-infiltrating CD8 T cells in situ. J. Immunol. 2016; 197:2509–2521. [PubMed: 27503208]

27. Redmond WL, Linch SN. Combinatorial immunotherapeutic approaches to restore the function of anergic tumor-reactive cytotoxic CD8^{+} T cells. Hum. Vaccin. Immunother. 2016:2519–2522. [PubMed: 27459422]

28. Linch SN, Kasiewicz MJ, McNamara MJ, Hilgart-Martiszus IF, Farhad M, Redmond WL. Combination OX40 agonism/CTLA-4 blockade with HER2 vaccination reverses T-cell anergy and promotes survival in tumor-bearing mice. Proc. Natl. Acad. Sci. U.S.A. 2016; 113:E319–E327. [PubMed: 26729864]

29. Bertoletti A, Ferrari C. Adaptive immunity in HBV infection. J. Hepatol. 2016; 64:S71–S83. [PubMed: 27084039]

30. Chang J, Guo F, Zhao X, Guo J-T. Therapeutic strategies for a functional cure of chronic hepatitis B virus infection. Acta Pharm. Sin. B. 2014; 4:248–257. [PubMed: 26579392]

31. Maini MK, Gehring AJ. The role of innate immunity in the immunopathology and treatment of HBV infection. J. Hepatol. 2016; 64:S60–S70. [PubMed: 27084038]

32. Shimizu Y. T cell immunopathogenesis and immunotherapeutic strategies for chronic hepatitis B virus infection. World J. Gastroenterol. 2012; 18:2443–2451. [PubMed: 22654441]

33. Yang N, Bertoletti A. Advances in therapeutics for chronic hepatitis B. Hepatol. Int. 2016; 10:277–285. [PubMed: 26363922]

34. Vilarinho S, Ogasawara K, Nishimura S, Lanier LL, Baron JL. Blockade of NKG2D on NKT cells prevents hepatitis and the acute immune response to hepatitis B virus. Proc. Natl. Acad. Sci. U.S.A. 2007; 104:18187–18192. [PubMed: 17991774]

35. Chisari FV, Filippi P, McLachlan A, Milich DR, Riggs M, Lee S, Palmiter RD, Pinkert CA, Brinster RL. Expression of hepatitis B virus large envelope polypeptide inhibits hepatitis B surface antigen secretion in transgenic mice. J. Virol. 1986; 60:880–887. [PubMed: 3783819]

36. Guidotti LG, Matzke B, Schaller H, Chisari FV. High-level hepatitis B virus replication in transgenic mice. J. Virol. 1995; 69:6158–6169. [PubMed: 7666518]

37. Pippig SD, Pena-Rossi C, Long J, Godfrey WR, Fowell DJ, Reiner SL, Birkeland ML, Locksley RM, Barclay AN, Killeen N. Robust B cell immunity but impaired T cell proliferation in the absence of CD134 (OX40). J. Immunol. 1999; 163:6520–6529. [PubMed: 10586044]

38. Chomczynski P. A reagent for the single-step simultaneous isolation of RNA, DNA and proteins from cell and tissue samples. Biotechniques. 1993; 15:532–534. [PubMed: 7692896]

39. Schneider CA, Rasband WS, Eliceiri KW. NIH Image to ImageJ: 25 years of image analysis. Nat. Methods. 2012; 9:671–675. [PubMed: 22930834]
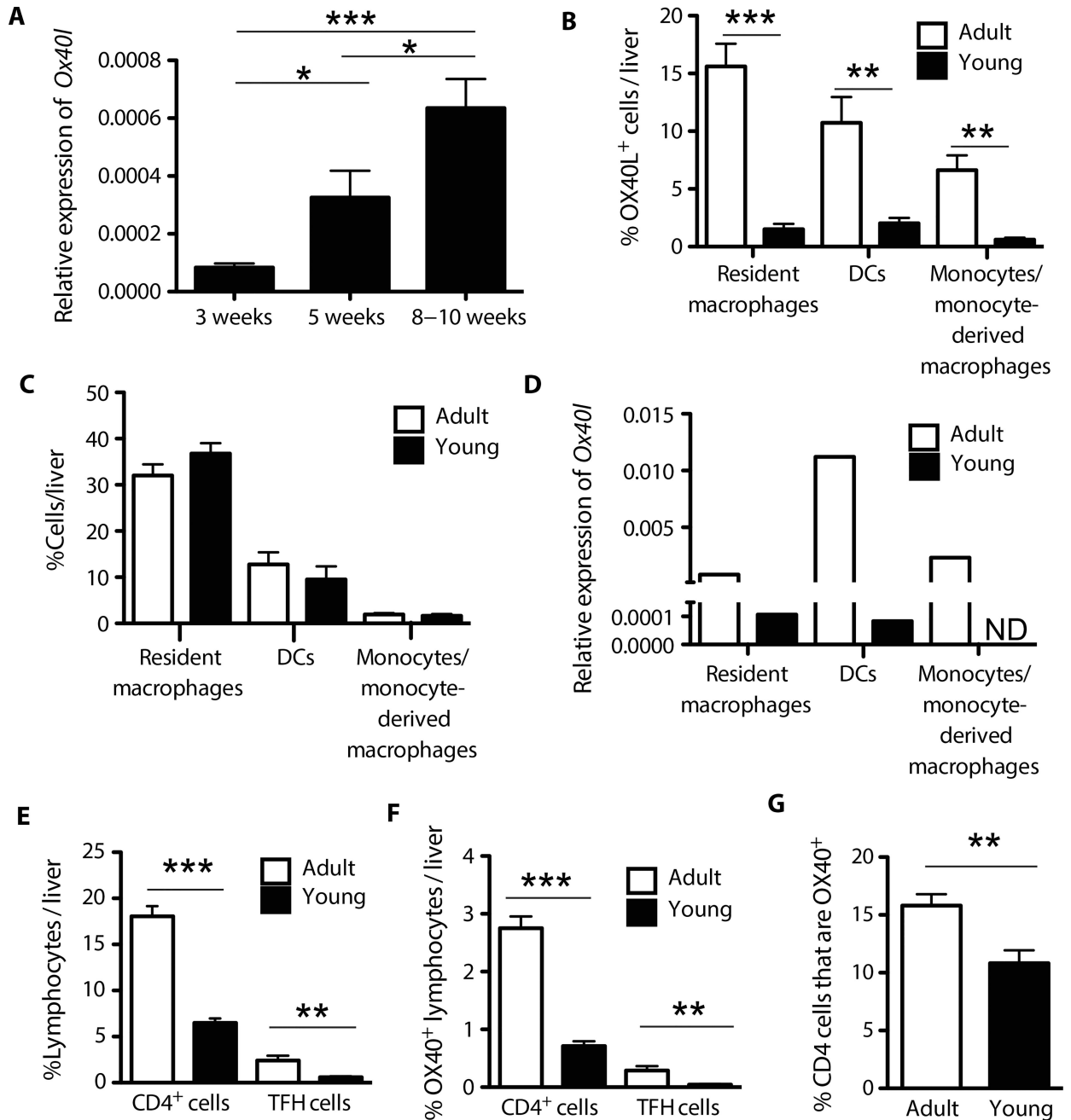
Fig. 1. Age-dependent expression of OX40 ligand on hepatic APCs and age-dependent expression of OX40 on liver-derived CD4$^+$ T cells during acute hepatitis

(**A**) *Ox40l* mRNA expression relative to *Gapdh* was determined by real-time polymerase chain reaction (RT-PCR) using mRNA derived from myeloid-enriched leukocyte preparations isolated from the liver of adult (8 to 11 weeks) and young (3 weeks) *Rag1$^{-/-}$* mice ($n = 10$). (**B** and **C**) Percentages of OX40L$^+$ (B) and percentages of all (C) resident macrophages [F4/80^{hi}, CD11b$^{+/intermediate(int)}$, major histocompatibility complex (MHC) class II$^{+/int}$, CD11c$^-$, Ly6G$^-$, Ly6C$^-$, and NK1.1$^-$], dendritic cells (DCs; CD11c$^{+/hi}$, MHC class II$^{+/hi}$, CD11b$^-$, Ly6G$^-$, Ly6C$^-$, and NK1.1$^-$), and monocytes/monocyte-derived macrophages (F4/80^{int}, CD11b$^{+/hi}$, MHC class II$^{+/int}$, Ly6C$^+$, Ly6G$^-$, CD11c$^-$, and NK1.1$^-$)

(n = 4). (**D**) *Ox40l* mRNA expression relative to *Gapdh* was determined by RT-PCR using mRNA derived from flow-sorted pooled cell populations from adult and young livers (n = 6 mice). ND, not detectable. (**E** to **G**) Lymphocytes were isolated from HBVEnvRag$^{-/-}$ mouse livers 8 days after adoptive transfer of splenocytes (n = 8). Flow cytometry was used to determine (E) percentages of CD4$^+$ T cells [CD4$^+$, T cell receptor β (TCRβ)$^+$, NK1.1$^-$, CD8$^-$, and CD19$^-$] and T follicular helper (T$_{FH}$) cells (CD4$^+$, TCRβ$^+$, CXCR5$^+$, ICOS$^+$, NK1.1$^-$, CD8$^-$, and CD19$^-$), (F) percentages of OX40$^+$ CD4$^+$ T cells and OX40$^+$ T$_{FH}$ cells, and (G) percentages of CD4$^+$ T cells that are also OX40$^+$ in the liver. Bars represent means ± SEM. Statistical significance was determined using the unpaired two-tailed *t* test (*$P <$ 0.05, **$P <$ 0.01, and ***$P <$ 0.001).
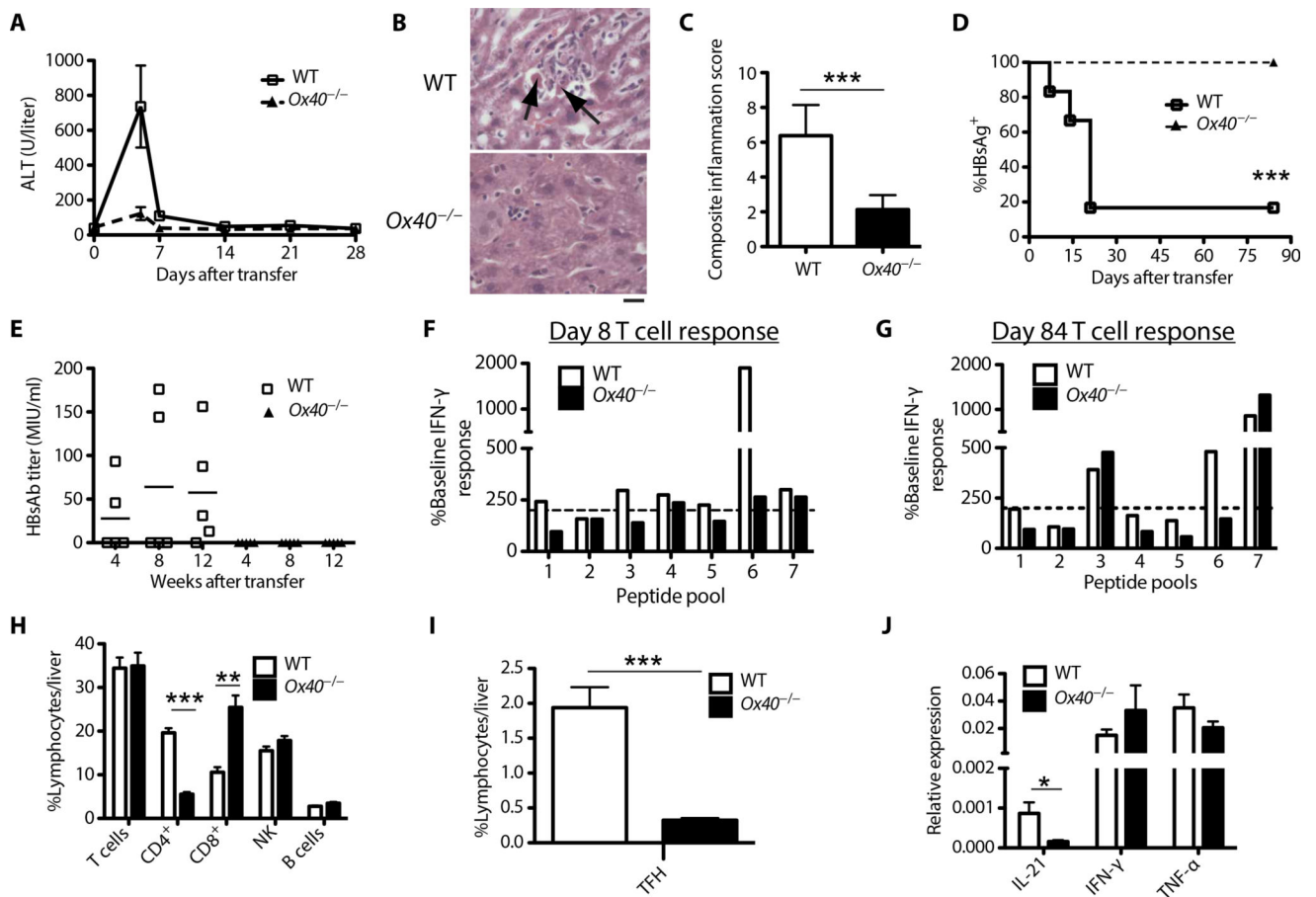
Fig. 2. Adoptive transfer of adult *Ox40*^{−/−} splenocytes into adult HBVEnvRag^{−/−} mice alters hepatic inflammation, HBsAg clearance, HBsAb seroconversion, T cell responses, and cytokine production

(**A**) Plasma alanine aminotransferase (ALT) values, reflecting liver injury, were determined for HBVEnvRag^{−/−} mice receiving wild-type (WT) (*Ox40*^{+/+}) splenocytes (open squares, solid line) or *Ox40*^{−/−} splenocytes (closed triangles, dotted line) at given time points after adoptive transfer (*n* 5). (**B**) Hematoxylin and eosin staining of liver sections from adult HBVEnvRag^{−/−} mice 8 days after adoptive transfer. Arrows indicate necrotic hepatocytes. Scale bar, 25 μm. (**C**) Composite score of hepatic necrosis, portal inflammation, and intraparenchymal inflammation in the liver sections determined by a pathologist blinded to sample identity. Statistical significance was determined using Mann-Whitney two-tailed (***P = 0.0008; *n* = 8 mice). (**D**) Plasma HBsAg loss and (**E**) HBsAb titer in HBVEnvRag^{−/−} mice at given time points after adoptive transfer. Statistical significance was determined using the chi-square test (***P < 0.001; *n* 5 mice). (**F** and **G**) Presence of hepatitis B virus (HBV)–specific T cells was determined using IFN-γ enzyme-linked immunospot (ELISpot) 8 days (F) and 84 days (G) after adoptive transfer (data pooled from *n* = 5 mice). Threshold defining a positive response is 2× the baseline (dashed line). (**H** and **I**) Percentages of total lymphocyte subpopulations were determined by flow cytometry in the liver 8 days after adoptive transfer: T cells are CD19^{−} and TCRβ^{+}; CD4^{+} T cells are CD4^{+}, CD8^{−}, TCRβ^{+}, and CD19^{−}; T$_{FH}$ cells are CD4^{+}, CD8^{−}, TCRβ^{+}, CD19^{−}, CXCR5^{+}, and ICOS^{+}; CD8^{+} T cells are CD4^{−}, CD8^{+}, TCRβ^{+}, and CD19^{−}; B cells are TCRβ^{−} and CD19^{+}; NK cells are

TCRβ⁻, CD19⁻, and NK1.1⁺. Statistical significance was determined using the unpaired two-tailed t test (**$P < 0.01$ and ***$P < 0.001$; $n = 5$ mice). Bars represent means ± SEM. (**J**) Expression of various cytokine mRNAs relative to *Gapdh* was detected by RT-PCR on mRNA from liver lymphocytes 8 days after adoptive transfer (n 5). Bars represent means ± SEM. Statistical significance was determined using the unpaired two-tailed t test (*$P < 0.05$).
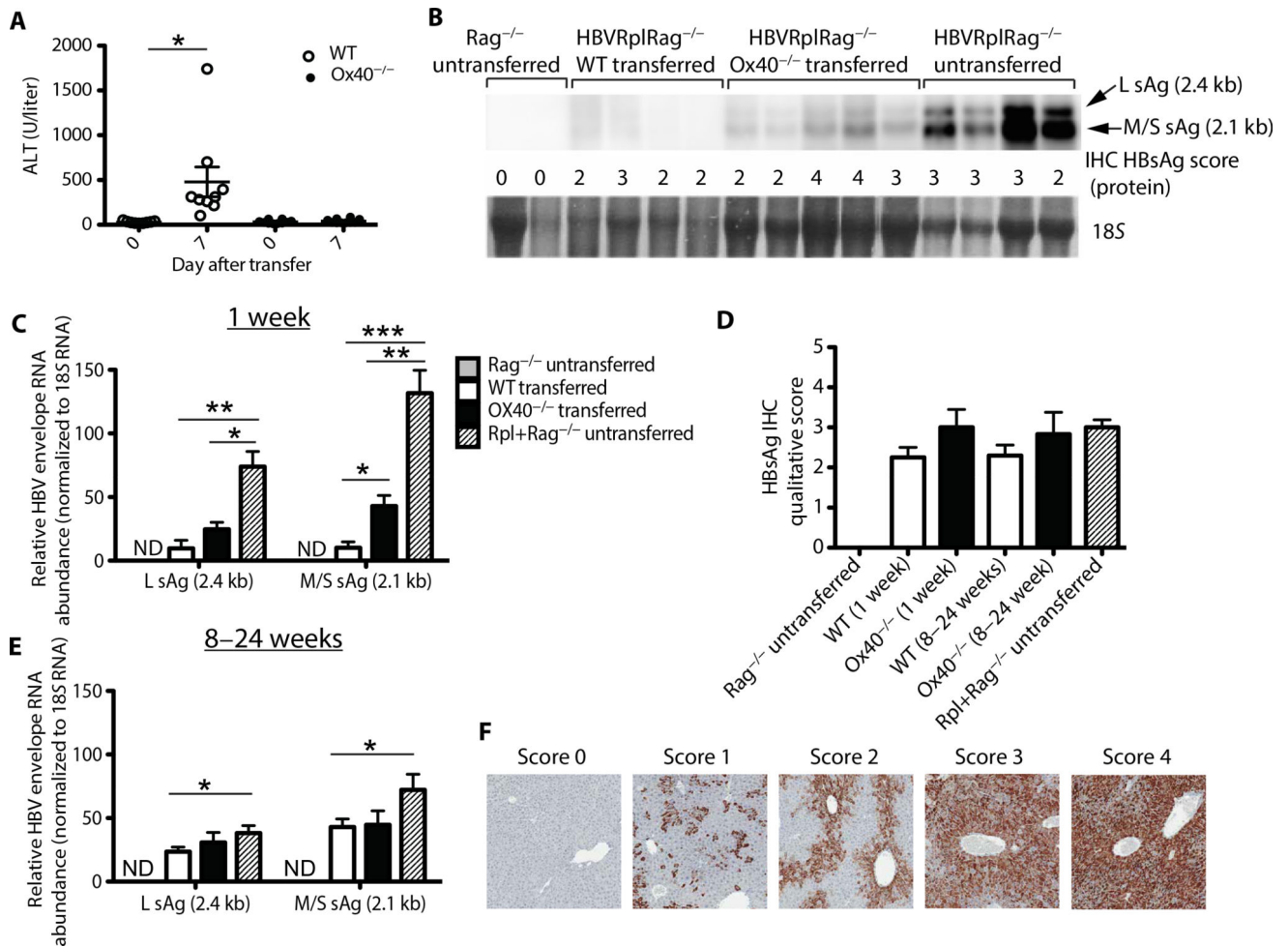
Fig. 3. Hepatic HBV envelope RNA and protein expression levels in HBVRplRag$^{-/-}$ mice 7 days (1 week) and 8 to 24 weeks after adoptive transfer with WT or *Ox40*$^{-/-}$ splenocytes show OX40-dependent regulation of viral replication intermediates

(**A**) Plasma ALT values, reflecting liver injury, were determined for HBVRplRag$^{-/-}$ mice receiving WT splenocytes (open circles) or *Ox40*$^{-/-}$ splenocytes (closed circles) at day 7 after adoptive transfer (*n*   9). Statistical significance was determined using the paired two-tailed *t* test (*$P < 0.05$). Liver pieces were removed 7 days (**B** to **D**), 8 weeks, or 24 weeks (D and **E**) after adoptive transfer and either flash-frozen for RNA extraction or fixed in formalin for immunohistochemistry (IHC). (C and E) HBV envelope RNA was detected by Northern blot analysis using a DIG-labeled (−) strand HBV RNA probe. RNA transcript band intensities in WT or *Ox40*$^{-/-}$ transferred mice were compared to untransferred *Rag1*$^{-/-}$ negative controls or untransferred HBVRplRag$^{-/-}$ positive controls and normalized to 18S RNA bands. Statistical significance was determined using the unpaired two-tailed *t* test (*$P < 0.05$; *n*   4 for all groups except Rag$^{-/-}$ untransferred, where $n = 2$). Bars represent means ± SEM. (D) HBV envelope protein levels were measured by IHC staining of formalin-fixed liver tissue with an HBsAg-specific antibody and counterstained with hematoxylin. Stained sections were scored by a pathologist blinded to sample identities using the scoring system shown in (F); 0, no staining; 1, multifocal granular or diffuse staining in hepatocytes involving <25% of section; 2, granular or diffuse staining around centrilobular hepatocytes

with no staining in portal regions; 3, diffuse positivity of hepatocytes restricted to centrilobular region; granular cytoplasmic positivity in remaining hepatocytes; and 4, diffuse positivity of hepatocytes restricted to centrilobular and mid zonal regions; granular cytoplasmic positivity in remaining hepatocytes. n ≥ 4 for all groups except Rag$^{-/-}$ untransferred, where $n = 2$. Bars represent means ± SEM.
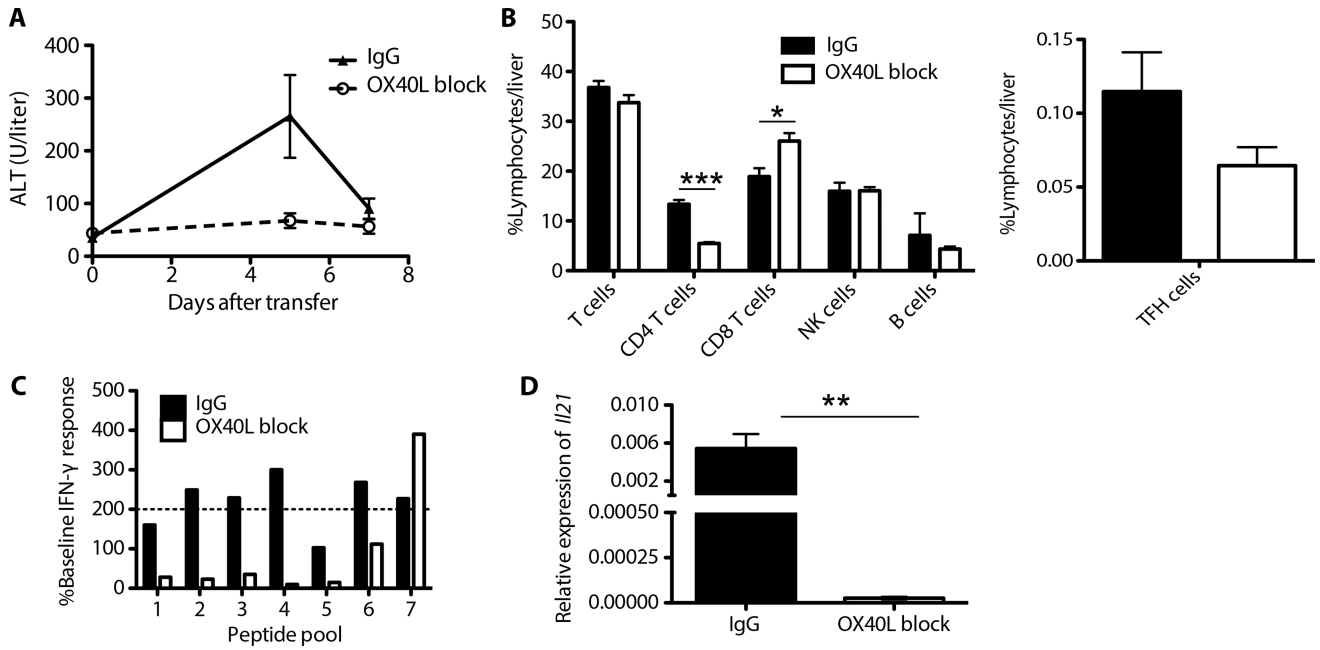
Fig. 4. Adoptive transfer of adult WT splenocytes into HBVEnvRag$^{-/-}$ adult mice treated with an OX40L blocking antibody abrogates biochemical hepatitis and HBV-specific T cell responses and cytokine expression

(**A**) Plasma ALT values were determined in HBVEnvRag$^{-/-}$ adult mice receiving intraperitoneal injection of 100 μg of OX40 ligand (OX40L) block (RM134L) (open circles, dotted line) or control IgG (purified rat IgG2b isotype control; closed triangles, solid line) on days 0, 2, 4, and 6 after adoptive transfer of WT splenocytes ($n = 7$). (**B**) Eight days after transfer, percentages of lymphocyte populations were determined by flow cytometric analysis of liver lymphocytes derived from HBVEnvRag$^{-/-}$ mice treated with either control IgG (black bars) or OX40L block (white bars). Bars represent means ± SEM. Statistical significance was determined using the unpaired two-tailed t test (*$P < 0.05$ and ***$P < 0.001$; $n = 6$). (**C**) HBV-specific T cell responses were measured using IFN-γ ELISpot assay 8 days after adoptive transfer. Threshold defining a positive response is 2× the baseline (dashed line; $n =$ pooled from four mice). (**D**) Relative *Il21* expression compared to *Gapdh* was detected by RT-PCR on mRNA from liver lymphocytes isolated 8 days after adoptive transfer. Bars represent means ± SEM. Statistical significance was determined using the unpaired two-tailed t test (**$P < 0.01$; $n = 6$).
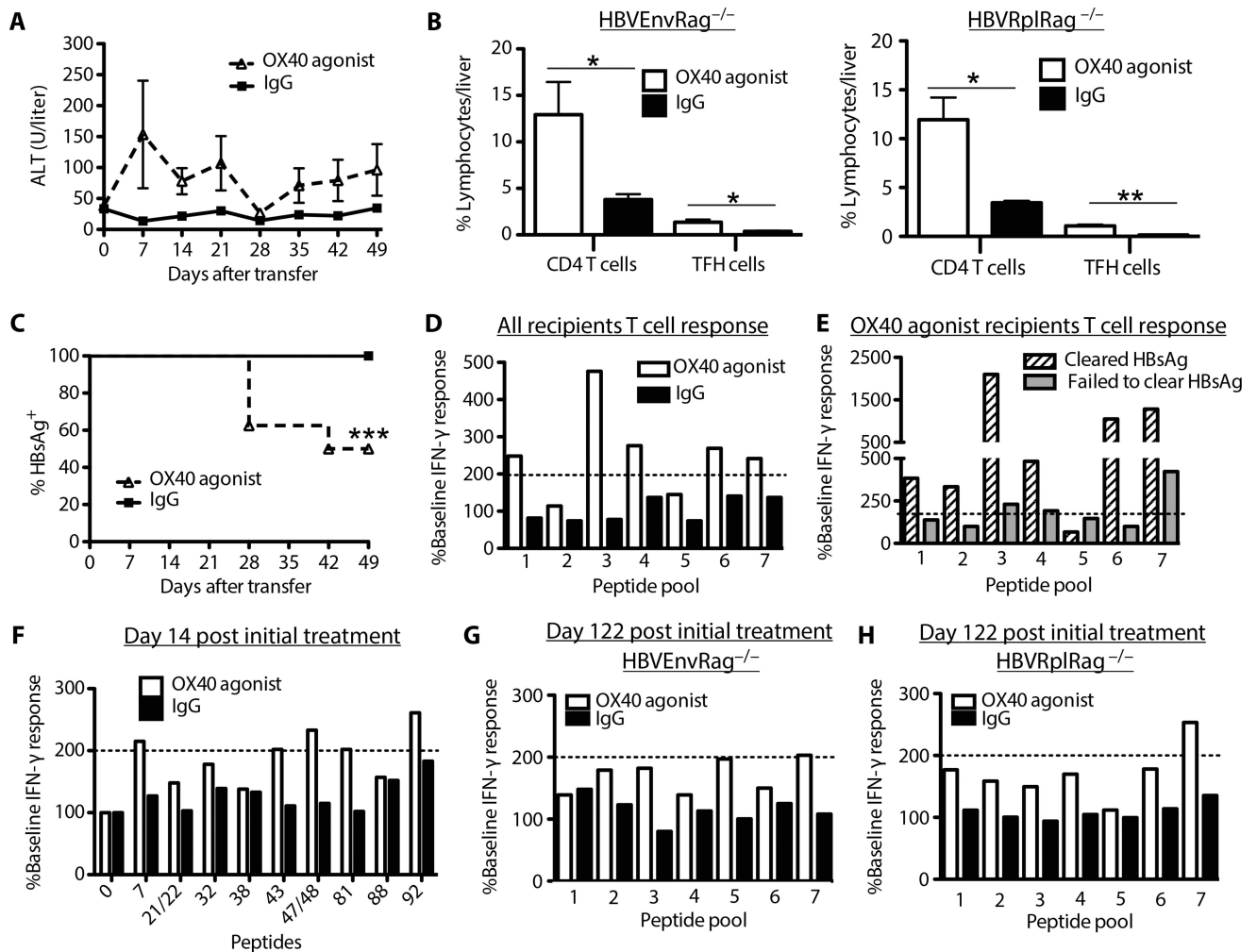
Fig. 5. Treatment with an OX40 agonist antibody of 3-week-old HBVtgRag$^{-/-}$ mice or mice with chronic HBV disease results in an altered immune response to HBV

(**A**) Plasma ALT values from young HBVEnvRag$^{-/-}$ mice receiving intraperitoneal injection of 150 μg of OX40 agonist antibody (OX86; open triangles, dashed line) or control IgG (purified rat IgG1 isotype control; closed squares, solid line) on days 0, 3, and 5 after adoptive transfer of WT splenocytes ($n = 4$). (**B**) Percentages of CD4$^+$ T cells and T_{FH} cells determined by flow cytometry in liver tissue 8 days after adoptive transfer into 3-week-old HBVEnvRag$^{-/-}$ (left panel) or HBVRplRag$^{-/-}$ (right panel) treated with control IgG (black bars) or OX40 agonist (white bars). Bars represent means ± SEM. Statistical significance was determined using the unpaired two-tailed t test (*$P < 0.05$ and **$P < 0.01$; n 3). (**C**) Presence of HBsAg in the plasma of young HBVEnvRag$^{-/-}$ mice treated with OX40 agonist (open triangles, dashed line) or control IgG (closed squares, solid line). Statistical significance was determined using the chi-square test (***$P < 0.001$). Data were pooled from two experiments ($n = 8$ mice per group total). (**D**) Presence of HBV-specific T cells was determined using IFN-γ ELISpot 56 days after adoptive transfer of young HBVEnvRag$^{-/-}$ mice injected with OX40 agonist (white bars) or control IgG (black bars). Data are representative of three individual experiments ($n =$ pooled from four mice). (**E**) IFN-γ ELISpot analysis of HBV-specific T cell responses on liver lymphocytes from mice treated

with OX40 agonist that cleared HBsAg (striped bars) or treated with OX40 agonist and did not clear HBsAg (gray bars) (n = pooled from two mice). For (D) and (E), the threshold defining a positive response is 2× the baseline (dashed line). (**F** to **H**) HBVRplRag$^{-/-}$ or HBVEnvRag$^{-/-}$ mice confirmed to have the serological profile of chronic HBV disease were treated with OX40 agonist (open bars) or control antibody (closed bars) (F) for eight treatments 3×/week or (G and H) at days 84, 87, 89 and 168, 171, 173, 175 after adoptive transfer. Presence of HBV-specific T cells was determined using IFN-γ ELISpot on liver lymphocytes after stimulation with (F) individually defined dominant and subdominant peptide epitopes or (G and H) pools of HBV peptides spanning the entire protein (F) 14 days or (G and H) 122 days after first treatment with OX40 agonist or control IgG (38 days after second treatment and 206 days after adoptive transfer) in (G) HBVEnvRag$^{-/-}$ mice and (H) HBVRplRag$^{-/-}$ mice. Data are representative of two individual experiments (n = pooled from 2–4 mice). Threshold defining a positive response is 2× the baseline (dashed line).
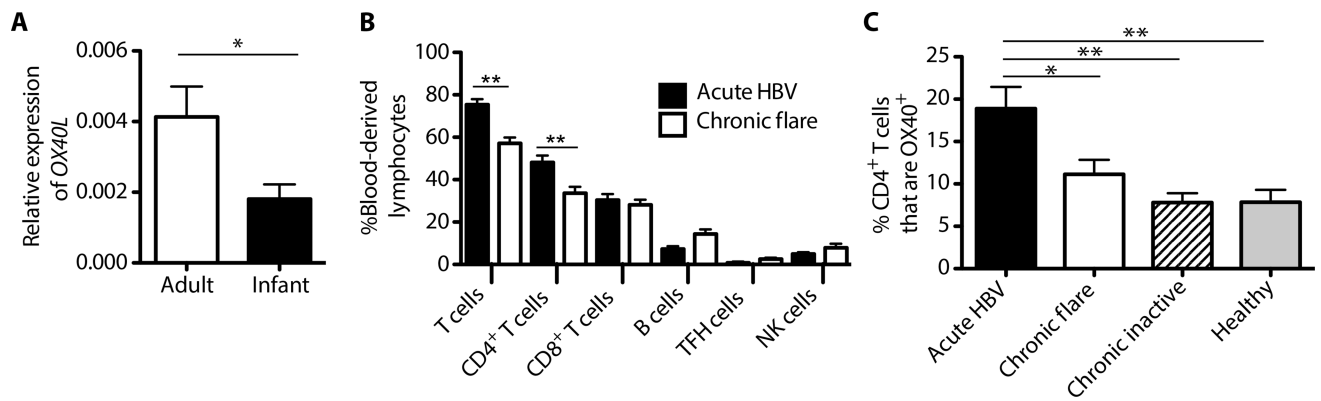
Fig. 6. Adult human liver shows greater *OX40L* expression than infant liver, and patients with acute hepatitis B who clear the virus have significantly increased percentages of PBMC-derived CD4+ T cells, a greater percentage of which express OX40

(**A**) Expression of *OX40L* relative to *GAPDH* was determined by RT-PCR performed on RNA extracted from paraffin-embedded liver biopsy samples from infants 6 to 12 weeks of age (black bar, $n = 24$) and adults (white bar, $n = 9$). Bars represent means ± SEM. Statistical significance was determined using the unpaired two-tailed *t* test (*$P < 0.05$). (**B**) Flow cytometry analysis comparing lymphocyte populations in PBMC obtained from eight patients with confirmed acute HBV infection during active hepatitis and with confirmed subsequent viral clearance and HBsAb seroconversion, and eight patients with confirmed chronic HBV infection exhibiting a flare of disease. T cells are TCRβ+, CD19−, and CD56−; CD4+ T cells are CD4+, CD8−, TCRβ+, and CD19−; T$_{FH}$ cells are CD4+, CD8−, TCRβ+, CD19−, CXCR5+, and ICOS+; CD8+ T cells are CD4−, CD8+, TCRβ+, and CD19−; B cells are TCRβ− and CD19+; and NK cells are TCRβ−, CD19−, CD56+, and CD16+. Bars represent means ± SEM. Statistical significance was determined using the unpaired two-tailed *t* test (**$P < 0.01$). (**C**) Percentage of CD4+ OX40+ T cells present in PBMC obtained from eight patients with acute HBV, eight patients with chronic HBV exhibiting a hepatitic flare of disease, as well as six untreated patients with confirmed chronic HBV with inactive disease (normal ALT), and six healthy individuals. Bars represent means ± SEM. Statistical significance was determined using Tukey's analysis of variance (ANOVA) multiple comparison test (*$P < 0.05$ and **$P < 0.01$).